Hindawi
Journal of Nanomaterials
Volume 2022, Article ID 5118455, 10 pages
https://doi.org/10.1155/2022/5118455

Research Article

Repair of Osteonecrosis of the Femoral Head with Adipose-Derived Stem Cell Composite with New Nanomaterial

Hanxiao Zhu, Bin Hu, Xiangfeng Zhang, Chenhe Zhou, and Cong Wang

Department of Orthopaedic Surgery, Second Affiliated Hospital, School of Medicine, Zhejiang University, Hangzhou, 310009 Zhejiang Province, China

Correspondence should be addressed to Cong Wang; 05wangcong@zju.edu.cn

Received 25 January 2022; Revised 16 May 2022; Accepted 17 May 2022; Published 8 July 2022

Academic Editor: Palanivel Velmurugan

This study was aimed at researching the effect of adipose-derived stem cell (ADSC) composite with new nanomaterials on repairing osteonecrosis of the femoral head (ONFH). Nanophase hydroxyapatite/collagen bone material was composited with ADSCs to form a new nanobone material. 24 bone defect rabbits were divided into S1 group (implanted with ADSC composite with nanophase hydroxyapatite/collagen bone material 14 days after modelling), S2 group (implanted with nanophase hydroxyapatite/collagen bone material), and S3 group (simple models). HE staining was used to measure the percentage area of trabecular bone and bone mineral density in rabbit femoral tissue, the load strength of femoral head was measured by orthopedic biomechanical tester, and the number of FVII-Ag-positive cells was detected by immunohistochemistry. There were 8 rabbit models in each group. ADSCs showed black nodules after alkaline phosphatase staining, which was a positive reaction. The OD value of ADSC cells showed a trend of increasing first and then decreasing. The growth rate of ADSC cells was relatively slow in 1-4 days, the growth rate was significantly accelerated in 4-6 days, and the growth inhibition period was entered after 6 days. After hematoxylin-eosin (HE) staining, many scattered bone trabecular structures and bone marrow tissues were found in the rabbits in the S1 group. The nanomaterials were still observed in the rabbits in the S2 group after surgery, and large sheets of bone trabecula appeared with the formation of medullary cavity partially. The bone marrow tissues of the rabbits in the S3 group disappeared partially after surgery, and undifferentiated mesenchymal stem cells and capillaries appeared with many scattered bone trabeculae. The rabbits in the S1 group had significantly higher trabecular bone percentage area and bone mineral density (59.76 ± 6.23; $0.141 \pm 0.015\,g/cm^2$) than the S2 group (42.51 ± 7.03; $0.113 \pm 0.008\,g/cm^2$), and the differences were statistically significant ($P < 0.05$). The postoperative load strength of rabbits in group S1 was significantly higher than that in group S2, and the difference was statistically significant ($P < 0.05$). ADSC composite with the new nanomaterial had a good repairing effect on ONFH.

1. Introduction

Osteonecrosis of the femoral head (ONFH) refers to a disease in which the blood supply of the femoral head is interrupted or damaged. It causes the death and subsequent repair of bone cells and bone marrow components, then leading to changes in the structure of the femoral head, collapse of the femoral head, and joint dysfunction. Also known as avascular necrosis of the femoral head, it is a common refractory disease in orthopedics [1–3]. There are many factors that cause ONFH, including hip trauma, glucocorticoids, and long-term drinking. According to different causes, it can be classified into traumatic ONFH and nontraumatic ONFH [4]. In the early stage, it is mainly manifested as pain of side buttocks, groin, or waist; radiating pain in the knee joint; and chills, asthenia, and soreness and tingling of the lower limbs [5]. These symptoms may persist and be gradually worsened, or they may disappear in a short term and have repeated attacks. In the middle and late stages, pain and stiffness are gradually increased, and claudication occurs [6, 7]. However, these early symptoms are not typical, which makes the difficulty of early detection and treatment greatly in the clinical practice. The current treatment for ONFH is mainly to prevent the

collapse of the femoral head and try to maintain the biological hip joint for a long time, which includes nonsurgical treatment and surgical treatment [8, 9]. Nonsurgical treatment is suitable for people with a small area of ONFH and no bone collapse. For more serious cases, surgical treatment is required.

Adipose-derived stem cells (ADSCs) are derived from the mesoderm during embryonic development. They are a type of adult stem cells with self-renewal and multidifferentiation potential. They can be induced to differentiate into a variety of cells of fat, bone, cartilage, pancreatic islet β cells, and myocardium under specific conditions, widely used in clinical practice [10–12]. Studies have shown that ADSCs can have an induced differentiation into chondrocytes in the microenvironment in vivo. With the proliferation and passage of chondrocytes, the therapeutic effect of cartilage repair is achieved, which provides a basis for the treatment of osteonecrosis [13]. With the development of nanotechnology, more and more nano-biomaterials have been developed and utilized [14]. Guo et al. [15] prepared a polyvinyl alcohol/nanohydroxyapatite/polyamide 66 biocomposite, which was used in the repair and treatment of articular cartilage and subchondral defects in rabbit knee joints. It was found that the nanocomposite has good histocompatibility and is a satisfactory substitute for articular cartilage and subchondral bone. Xiong et al. [16] analyzed the repair effect of porous nanohydroxyapatite/polyamide 66 (n-HA/PA66) composites on bone defects and firstly performed biosafety experiments. The porous n-HA/PA66 composite material had no cytotoxicity, no sensitization, and no thermogenic reaction, and the hemolysis rate was less than 5%. The material was applied to a rabbit model of tibial defect, which finally showed that the porous n-HA/PA66 composite had good biosafety, good biocompatibility, osteoinduction, and osseointegration. Nanophase hydroxyapatite/collagen bone, as a new nanobone material, has been approved for clinical treatment; and its crystal composition and size are very close to those of natural bone. Thus, it can provide a more natural microenvironment to help bone cells grow, proliferate, and adhere, having splendid bone repair performance [17]. Therefore, 24 healthy New Zealand white rabbits were selected as research samples, rabbit ADSC cells were isolated and cultured, and a rabbit model of femoral head necrosis was constructed. The rabbits were divided into S1 group (implanted with ADSC composite with nanophase hydroxyapatite/collagen bone material 14 days after modelling), S2 group (implanted with nanophase hydroxyapatite/collagen bone material), and S3 group (simple models), with 5 rabbits in each group. Finally, the load strength of the three groups of rabbit femoral head and the number of FVII-Ag-positive cells and HE staining were analyzed to comprehensively explore the repairing effect of ADSC cells combined with new nanomaterials on femoral head necrosis, so as to provide further reference for the treatment of osteonecrosis.

2. Materials and Methods

2.1. Research Animals. 24 healthy New Zealand white rabbits purchased from the animal experiment center were selected as the research samples, with the weight of 2 ± 0.2 kg of each one. They were given normal water and food and raised in an environment of 25°C and 65% relative humidity. The animal processing and experimental procedures in this study conformed to the national laboratory animal standards and had been approved by the ethics committee.

2.2. Cell Isolation and Culture of Rabbit ADSCs. The operating steps were described as follows. After anesthetization, the paradidymal fat of the rabbits was taken, and the small blood vessels and fascia in the fat were removed. Then, the fat was washed with phosphate buffer solution (PBS) (Wuhan Proceeds Life Technology Co., Ltd., China) and cut into pieces. 0.16% type I collagenase (Nanjing Xinfan Biotechnology Co., Ltd., China) with 2 times of the volume was added to the fat, and it was incubated with shaking at 37°C for 50 minutes. Dulbecco's modified eagle medium/nutrient mixture F-12 (DMEM-12) medium (Suzhou Meilun Biotechnology Co., Ltd., China) was used to stop the culture, and 155 mM ammonium chloride (Ammonium Chloride, Zhejiang Longsheng Group Co., Ltd., China) was added after filtering. It was incubated at 37°C for 15 minutes and then was centrifuged at 2500 r/min for 20 minutes. After being washed with PBS, it was centrifuged again to collect the precipitated cells. The collected cells were inoculated in 4 mL DMEM-12 culture solution and were cultured in an incubator at 37°C with 5% carbon dioxide (CO_2). The culture medium was changed every two days. When the cells grew to about 85% to fuse, they were washed with PBS, and then, 1 mL trypsin/ethylenediaminetetraacetic acid (EDTA) (0.25%/0.02%) mixture was added. It was waited for 5 minutes, and DMEM-12 medium containing serum was added to shut down the culture. The obtained thing was centrifuged at 1200 r/min for 5 minutes, and the supernatant was aspirated. An appropriate amount of DMEM-12 medium was then added for subculture. When the cells were cultured to the third generation, dexamethasone at a concentration of 10^{-8}/mol, sodium glycerophosphate (Tianjin Jinyao Group Co., Ltd., China) at 8 mmol/L, and ascorbic acid (Hubei Nona Technology Co., Ltd., China) at 45 μg/mL were added to obtain the osteoblast culture medium.

2.3. Detection of Proliferation Activity of ADSC Cells. The growth and morphological characteristics of ADSCs were observed under a microscope.

The cell viability was detected by the tetramethylazolyl salt (MTT) (Shanghai Jining Industrial Co., Ltd., China) method, which followed the steps below. The third-generation ADSC cell was prepared into a single suspension, and the concentration was adjusted to be 1×10^6/mL. It was inoculated in a 16-well plate, with 1 mL in each well. After one day, the culture medium in the wells was aspirated, and MTT in a concentration of 5 mg/mL was added. It was then incubated for 5 hours at 37°C with 5% CO_2. After the MTT solution was aspirated, 1 mL trypsin/EDTA (0.25%/0.02%) mixed solution was added for digestion, and then, it was centrifuged at 1200 r/min for 5 minutes. 700 μL dimethyl sulfoxide (DMSO) (Shanghai Baijin Chemical Group Co., Ltd., China) solution was added into each

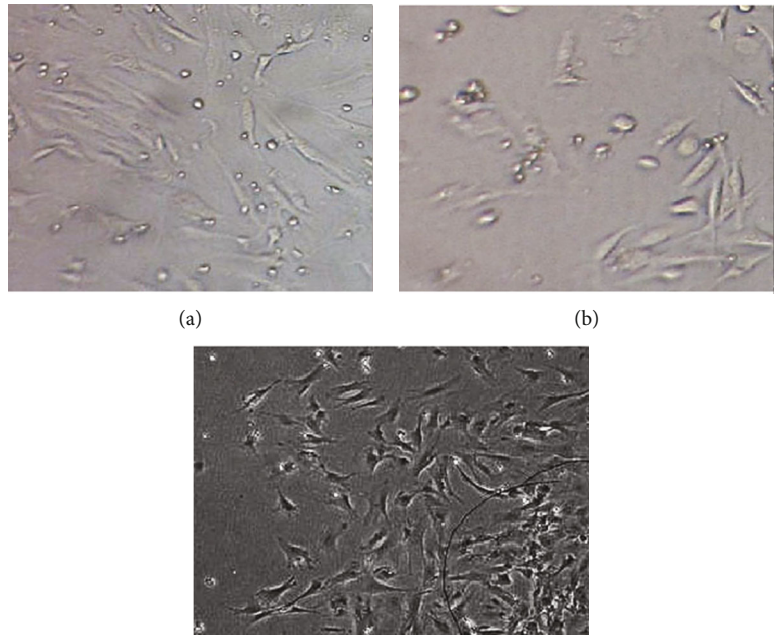

(a) (b) (c)

Figure 1: Microscopic observation results of ADSCs (400×). ((a)–(c) showed the cells on the first day of primary culture, the cells on the third day of primary culture, and the third-generation ADSCs, respectively).

sample well and was shaken for 15 minutes at 25°C to fully dissolve and mix well. Distilled water was used for zeroing, then the optical density (OD) value was measured at 450 nm, and the cell growth curve of ADSCs was drawn.

2.4. Fusion of ADSCs and Nanophase Hydroxyapatite/Collagen Material. The nanomaterials were prewetted and placed in a 16-well plate. The third-generation ADSCs, with a concentration adjusted to 1×10^6/mL, were inoculated on the nanomaterials. 120 minutes later, 2 mL DMEM-12 culture medium was added. An inverted microscope was used to observe the growth of cells in nanomaterials.

2.5. Construction and Administration of Rabbit ONFH Models. The 24 rabbits were divided into groups S1, S2, and S3, with 8 rabbits in each group. The rabbits in the S1 group were implanted with ADSC composite with nanophase hydroxyapatite/collagen material 14 days after the models were made. Those in the S2 group were implanted with nanophase hydroxyapatite/collagen bone material 14 days after the modelling, and those in the S3 group were simple models merely.

The rabbits were anesthetized with 25 mg/kg sodium pentobarbital (Shanghai Weijin Biotechnology Co., Ltd., China) via an ear vein injection. The fur on the left hip was shaved, and then, the position was disinfected with iodine. A 5 cm long wound was cut on the posterior hip joint, as it was completely cut open from the skin surface to the joint capsule. After dislocation of the femoral head, the retinaculum for blood supply was disconnected, and then, the hip joint was reset and sutured. After the surgery, the drugs of 450,000 U/kg were injected intramuscularly every day for 1 week.

14 days after modelling, the rabbits in the S3 group were not treated. After the rabbits in the S1 and S2 groups were anesthetized, the femoral head was exposed from the original incision on hip joint. A window with the size of 3×3 mm was made under the femoral head with X-ray imaging. From the window, the necrotic bone tissues were removed. It was best to implant ADSCs with nanophase hydroxyapatite/collagen material in rabbits in the S1 group and implant the nanophase hydroxyapatite/collagen material in those in the S2 group.

2.6. Observation of the Therapeutic Effect. For animal general observation, the life status and wound healing of rabbits were recorded at 1, 3, 5, and 7 weeks after surgery.

For morphological observation, tissue specimens were taken after the rabbits were killed. The tissues were fixed with neutral formalin solution and made into paraffin-embedded sections. The sections were processed with hematoxylin-eosin (HE) staining and then were observed under a high-definition microscope to measure the area ratio of bone trabecula and bone mineral density.

In terms of biomechanics, MX-0580-orthopedic biomechanics tester (produced by Shanghai Hengyi Precision Instrument Co., Ltd.) was used to measure the loading intensity of the femoral head.

The number of FVII-Ag-positive cells was counted through immunohistochemical staining: with xylene and 100% absolute ethanol, the tissue sections were put in distilled water. They were taken out, wiped dry, and placed in 0.3% hydrogen peroxide (H_2O_2) solution for 20 minutes. Then, they were washed with distilled water and soaked in PBS. After that, the sections were placed in the blocking solution for 15 minutes. As they were wiped dry, first

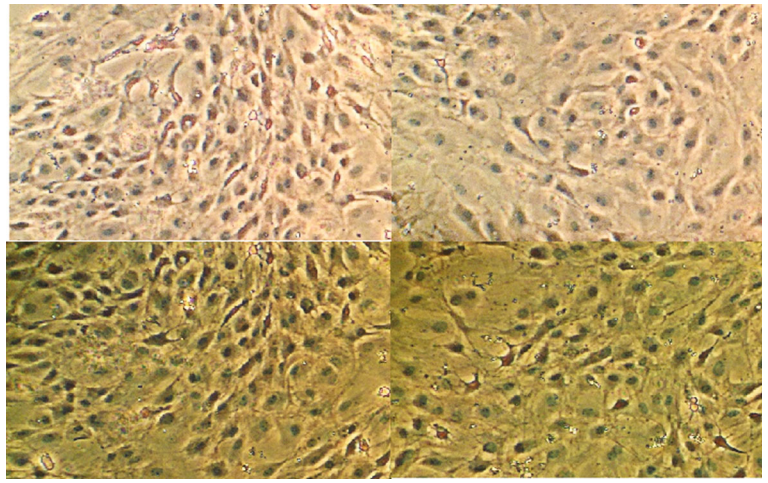

Figure 2: Alkaline phosphatase staining results of ADSCs (100×).

antibody solution was dropped on them. After overnight at 4°C, the sections were washed and infiltrated with PBS. Then, the secondary antibody was added dropwise. After 15 minutes at 37°C, they were washed and infiltrated with PBS again. Streptavidin-peroxidase solution was added dropwise, and the sections were placed for 15 minutes at 37°C. After PBS was added, they were placed again for 15 minutes at 37°C. 3,3′-Diaminobenzidine color developing solution was then added dropwise, and they were incubated at 25°C for 15 minutes. After being washed with water, the sections were counterstained with hematoxylin for 2 minutes. They were dehydrated with gradient alcohol and became transparent with xylene and then were fixed with neutral gum and sealed. Ten fields of view were selected under a high-definition microscope, to observe and record the number of FVII-Ag-positive cells. The average value was also calculated.

2.7. Statistical Methods. The data in this study was processed by SPSS19.0. The measurement data were expressed by the mean ± standard deviation ($\bar{x} \pm s$), and the enumeration data were expressed by percentage (%). Pairwise comparisons were performed by one-way analysis of variance, and the difference was statistically significant as $P < 0.05$.

3. Results

3.1. Microscope Observation Results of ADSCs. Figure 1 showed the microscopic observation results of ADSCs. It was observed that a small number of ADSCs had grown from the original mononuclear cells to spindle cells, and small colonies formed 1 day after primary culture. Three days after primary culture, the number of ADSCs increased significantly. The cells grew into a long spindle shape, with clear boundaries between nucleus and cytoplasm and larger colonies. The cultured third-generation ADSCs became larger and linked each other to form colonies; a large number of the cells tended to aggregate in a spiral arrangement.

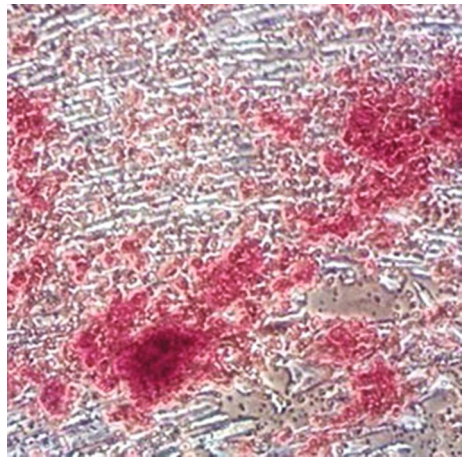

Figure 3: Alizarin red staining results of calcium nodules in ADSCs (100×).

3.2. Cell Staining Results of ADSCs. Figure 2 showed the results of alkaline phosphatase staining of ADSCs. Black nodules were observed in the ADSCs after alkaline phosphatase staining, which was a positive reaction.

The alizarin red staining results of calcium nodules in ADSCs were shown in Figure 3. The calcium nodules in ADSCs were bright red, and there were adherent osteoblasts around the calcium nodules. The cells were spindle-shaped and polygonal with purple-brown particles inside.

3.3. Cell Viability of ADSCs. Figure 4 showed the cell growth curve of ADSCs. The OD value of ADSCs first increased and then decreased. The growth of ADSCs was relatively slow in 1-4 days and was significantly accelerated in 4-6 days. After 6 days, it entered the growth inhibition period after 6 days.

3.4. Morphological Observation of Femoral Head Tissues of Rabbits in the Three Groups. From the results of HE staining of the femoral head tissues of rabbits in Figure 5, it was observed that the bone marrow tissues of the rabbits in the S3 group had partially disappeared after surgery.

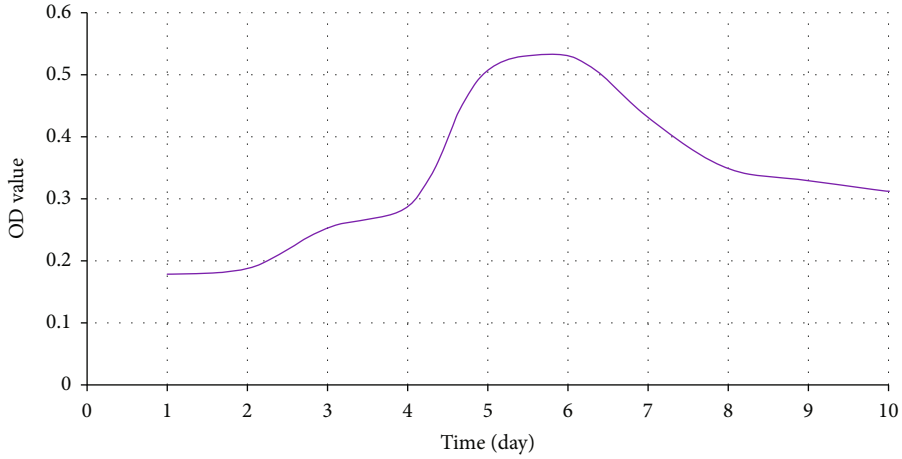

Figure 4: Cell growth curve of ADSCs.

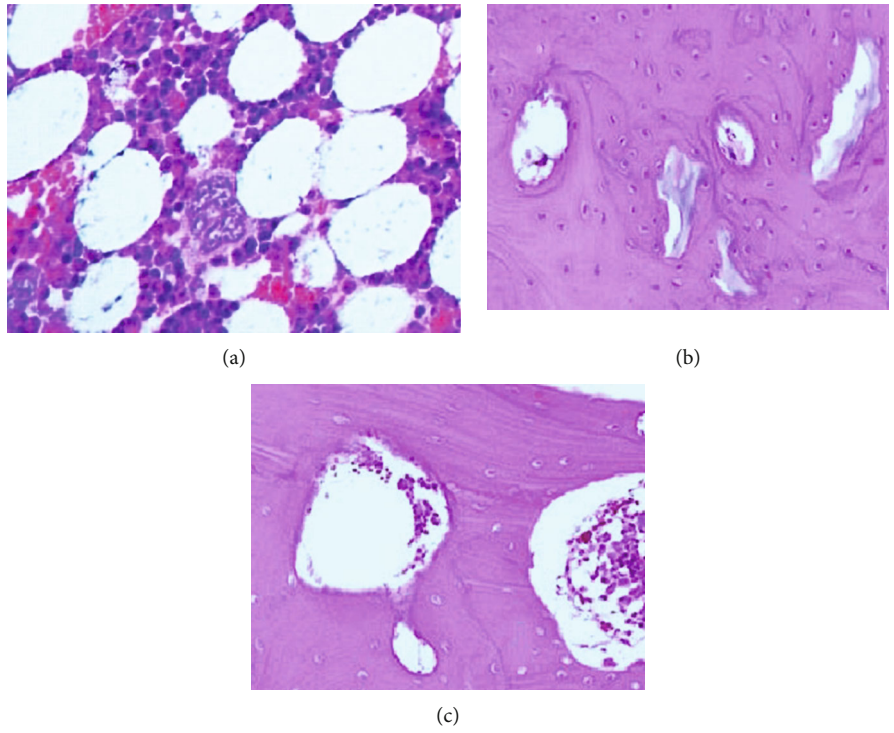

Figure 5: HE staining of rabbit femoral head tissues in three groups (100×). Note: (a)–(c) represented the S1 group, S2 group, and S3 group, respectively.

Undifferentiated mesenchymal stem cells and capillaries had appeared, and there were many scattered bone trabeculae. For the rabbits in the S2 group, the nanomaterial could still be observed after surgery, the blood vessels were reduced, large sheets of bone trabeculae appeared, and medullary cavity formed in some parts. In the S1 group, the nanomaterial was basically absorbed after surgery, and a large amount of scattered bone trabecular structure was observed, and the bone marrow tissue repair was formed.

3.5. General Conditions of Rabbits in the Three Groups after Surgery. The observation results of the general conditions of rabbits in the three groups after surgery were shown in Figure 6. It could be observed that the surface of the femoral head was obviously pale and the cartilage tissue was obviously defective in the S3 group. The femoral head in the S2 group was round, the surface was not smooth enough, and red cartilage tissues appeared, but the degree of defect was low. The surface of the femoral head in the S1 group was slightly pale, the surface was relatively smooth, red cartilage tissues appeared, and the size did not change.

3.6. Comparison of the Number of FVII-Ag-Positive Cells of Rabbits in the Three Groups after Surgery. Figure 7 showed

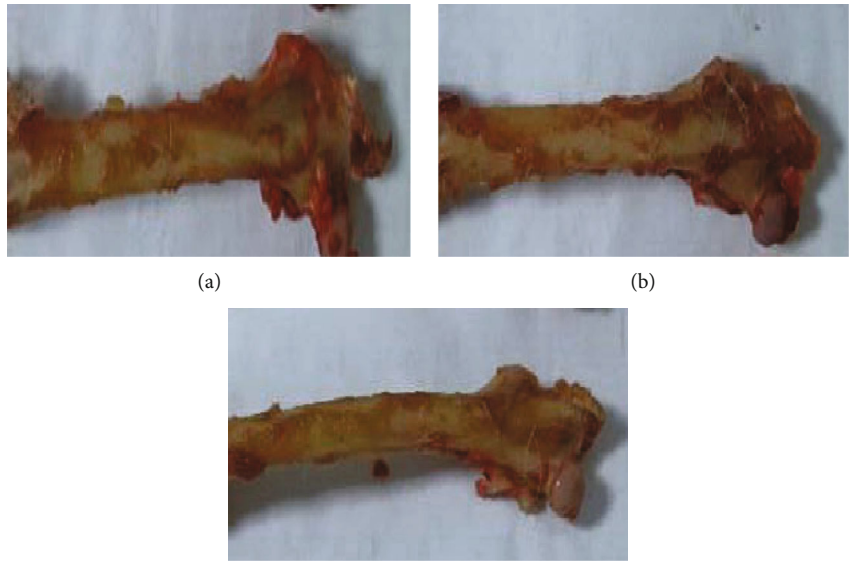

Figure 6: Observation results of the general conditions of rabbits in the three groups after surgery. Note: (a)–(c) represented the S1, S2, and S3 groups, respectively.

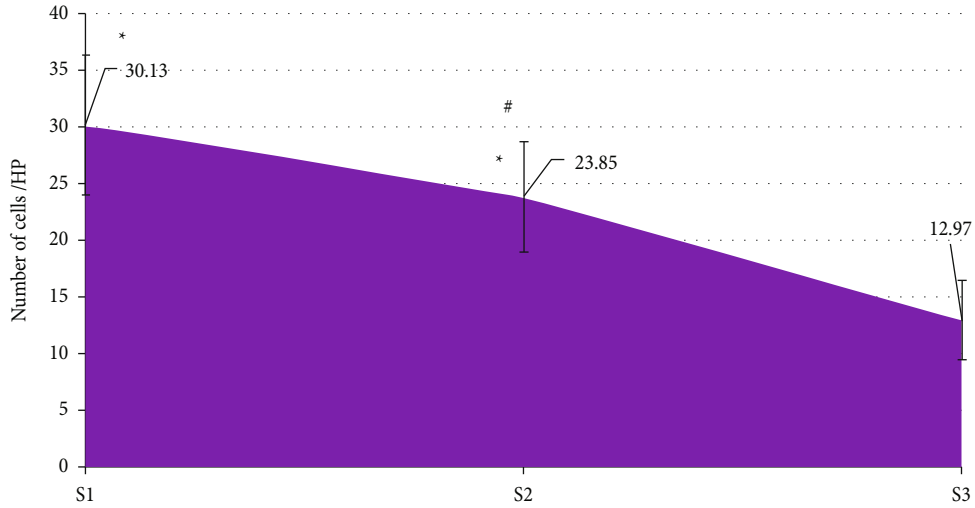

Figure 7: Comparison of the number of FVII-Ag-positive cells in the three groups after surgery. Note: ∗ and # indicated the statistically significant difference compared to the data in the S3 group and that in the S1 group, respectively ($P < 0.05$).

the distribution of FVII-Ag-positive cells of rabbits in the three groups after surgery. The number of FVII-Ag-positive cells of the rabbits in the S1 and S2 groups was significantly higher than that in the S3 group, and the difference was statistically significant ($P < 0.05$). Besides, the number of FVII-Ag-positive cells in the S1 group after surgery was significantly higher than that in the S2 group, with the statistically significant difference ($P < 0.05$).

3.7. The Area Ratio of Bone Trabecula and Bone Mineral Density of Rabbits in the Three Groups after Surgery. Figure 8 showed the comparison of the area ratio of the bone trabecula and bone mineral density after surgery of rabbits in the three groups. The area ratio of the bone trabecula and bone mineral density in the S1 and S2 groups were significantly higher than those in the S3 group, and the differences were statistically significant ($P < 0.05$). The rabbits in the S1 group had significantly higher trabecular bone percentage area and bone mineral density (59.76 ± 6.23; 0.141 ± 0.015 g/cm2) than the S2 group (42.51 ± 7.03; 0.113 ± 0.008 g/cm2), and the differences were statistically significant ($P < 0.05$).

3.8. Comparison of Postoperative Loading Intensity of Rabbits in the Three Groups. It was shown in Figure 9 that the postoperative loading intensity of the rabbits in the S1

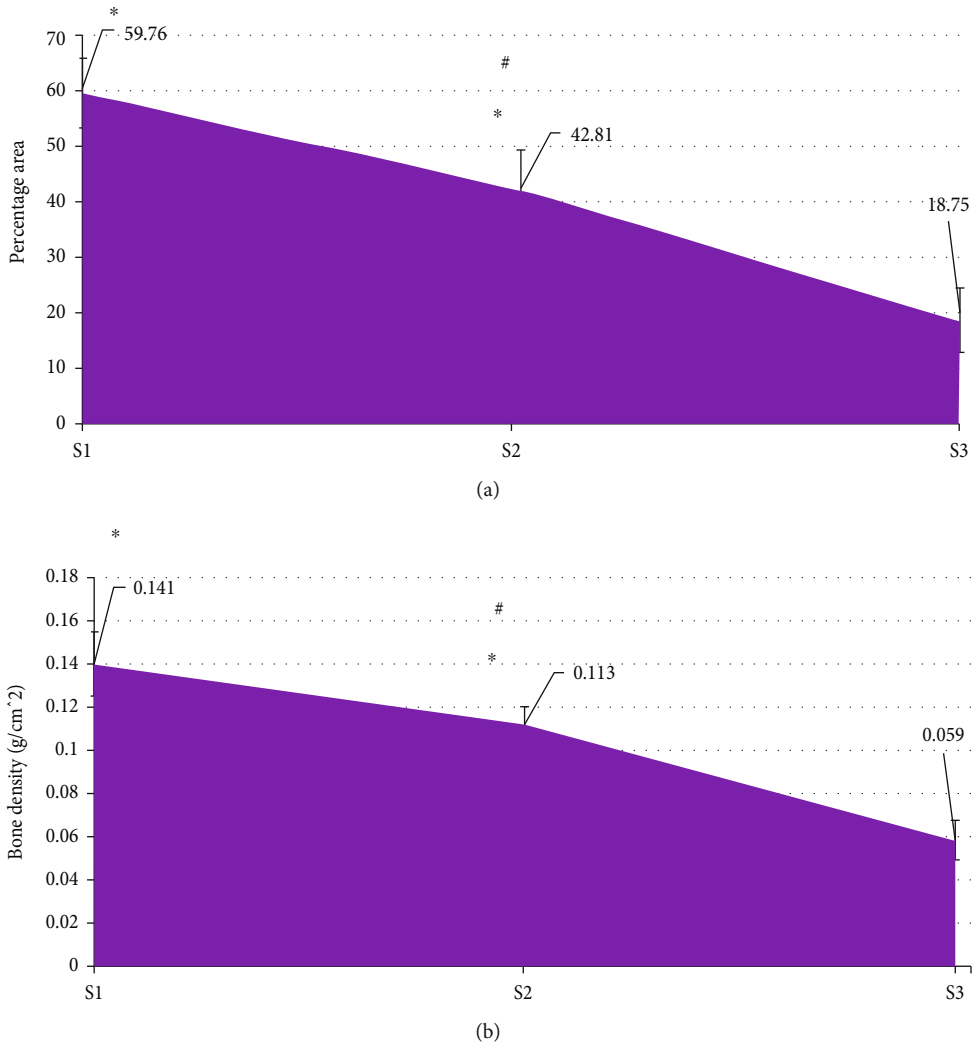

Figure 8: Comparison of area ratio of bone trabecula and bone mineral density of rabbits in the three groups after surgery. Note: * indicated that the differences were statistically significant compared with those in the S3 group ($P < 0.05$), while # indicated the statistically significant differences compared with those in the S1 group ($P < 0.05$).

and S2 groups was significantly higher than that in the S3 group, as the differences were statistically significant ($P < 0.05$). The loading intensity of the S1 group rabbits was significantly higher than that in the S2 group as well, and the difference was statistically significant ($P < 0.05$).

4. Discussion

ADSCs is a type of new seed cells with the advantages of strong reversibility, easy access, and no immune rejection, and it is an important research technology in bone tissue repair currently [18]. Clinical filling materials for bone defect repair include autologous bone, xenogeneic bone, and artificial bone. The artificial bone can serve as a scaffold and avoid the insufficient bone repair, now it is combined with nano-biomaterials in clinical treatment [19–21]. In this study, the nanophase hydroxyapatite/collagen bone material was selected and fused with ADSCs to form a new nanobone material. 24 New Zealand white rabbit bone defect models were divided into S1, S2, and S3 groups with 8 rabbits in each group. The rabbits in S1 group were implanted with ADSC composite with nanophase hydroxyapatite/collagen bone material 14 days after modelling. Only the nanophase hydroxyapatite/collagen bone material was implanted in the rabbits in S2 group 14 days after the model were papered. The S3 group was the simple model group. Firstly, the results of isolation and culture of rabbit ADSCs were analyzed. It was found that a small number of ADSCs had grown from the original mononuclear cells to spindle cells 1 day after primary culture, and small colonies formed. Three days after culture, the number of ADSCs increased greatly and the cells grew to be long fusiform with clear nuclei and cytoplasmic boundaries, and larger colonies formed. The third-generation ADSCs were linked in the form of colonies, and a large number of cells had a tendency to aggregate in a spiral distribution. The results were similar to the previous results obtained from ADSCs culture, indicating that the targeted induction culture of osteoblasts with

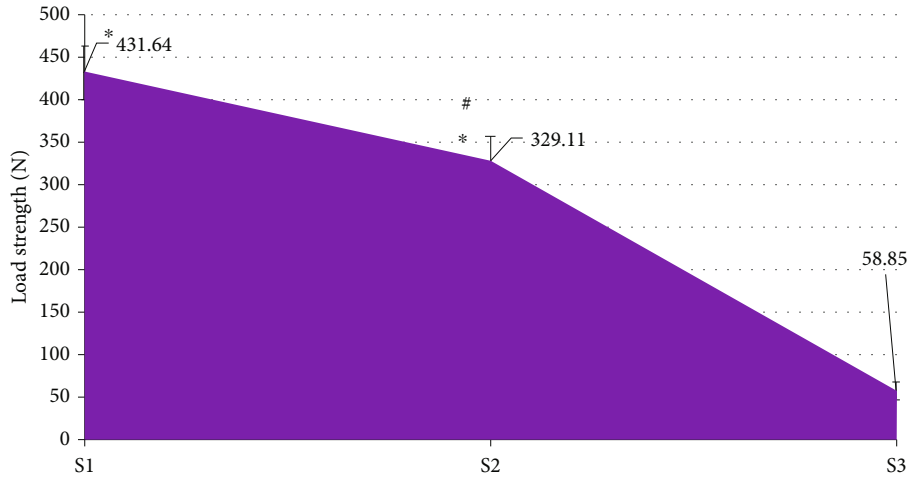

Figure 9: Comparison of postoperative loading intensity of rabbits in three groups. Note: ∗ indicated the statistically significant differences compared with that in the S3 group ($P < 0.05$); # indicated that the difference was statistically significant compared with that in the S1 group ($P < 0.05$).

rabbit ADSCs in this study was relatively successful [22]. Alkaline phosphatase belongs to phosphate monoester hydrolase, a group of specific phosphatases. It is widely distributed in human tissues and body fluids and can reflect the degree of differentiation from cells into osteoblasts [23]. It was found in this study that ADSCs showed black nodules after alkaline phosphatase staining, which was a positive reaction showing that ADSCs were more mature for osteoblast differentiation.

The postoperative conditions of rabbits in the three groups were compared; it was first discovered that a great many scattered bone trabecular structures and bone marrow tissue repair were in rabbits in the S1 group after surgery. In the S2 group, nanomaterials still existed, blood vessels reduced, large pieces of bone trabeculae appeared, and the medullary cavity was formed in some parts after surgery. The bone marrow tissues of the rabbits in the S3 group disappeared partially after surgery, and undifferentiated mesenchymal stem cells and capillaries appeared together with many scattered bone trabeculae. The HE staining results proved that the repairing effect of ADSC composite with nanophase hydroxyapatite/collagen material was better than that of single nanophase hydroxyapatite/collagen material on rabbit ONFH models [24]. The postoperative area ratio of bone trabecula and bone mineral density of rabbits in both S1 and S2 groups were greatly higher than those in the S3 group, while those in the S1 group were also higher than those in the S2 group, and all the differences were statistically significant ($P < 0.05$). This was indicated that both ADSC composite with nanophase hydroxyapatite/collagen bone material and single nanophase hydroxyapatite/collagen bone material could have a significant repairing effect on ONFH in rabbits. However, the repairing effect and degree of calcification of ADSC composite with nanophase hydroxyapatite/collagen material were better than those of the single nanophase hydroxyapatite/collagen material [25]. Bone biomechanical characteristics are indicators that directly reflect the quality of bone tissues [26]. In this study, the postoperative loading intensity of rabbits in the S1 and S2 groups was significantly higher than that in the S3 group, while that in the S1 group was significantly higher than that in the S2 group, as the differences were of statistical significance ($P < 0.05$). This was suggested that ADSC composite with nanophase hydroxyapatite/collagen material was better than single nanophase hydroxyapatite/collagen material in the microstructure of bone tissues.

5. Conclusion

In this work, nanophase hydroxyapatite/collagen bone material was fused with ADSC cells to form a new nanobone material, which was then applied to the treatment of bone defect in New Zealand white rabbits. Finally, it was found that both ADSC composite with nanophase hydroxyapatite/collagen material and the single nanophase hydroxyapatite/collagen material had obvious repairing effects on ONFH in rabbits. But ADSC composite with nanophase hydroxyapatite/collagen bone material had the better repairing effect as well as bone mineral quality than the single nanobone material. However, there were still some deficiencies in this study that needed to be improved. Only the effect of ADSC composite with nanophase hydroxyapatite/collagen material in bone repair was discussed, without the further analysis of the optimal dosage of nanobone composite material. Therefore, in the follow-up research, it would continue to select animal experimental samples, compare the different dosages of the nanomaterials, and analyze the optimal dosage of nanomaterials. In short, the results of this study gave a reference for the application of ADSC composite with nanomaterials in bone repair.

Data Availability

The data used to support the findings of this study are included within the article.

Conflicts of Interest

The authors declare that they have no competing interest.

Acknowledgments

This work was supported by the Zhejiang Natural Youth Fund, Project Name "Study on the molecular mechanism of eda-a2/eda2r molecule in hormone induced osteoporosis" (No. LQ18H070002).

References

[1] Z. L. Wang, R. Z. He, B. Tu et al., "Drilling combined with adipose-derived stem cells and bone morphogenetic Protein-2 to treat femoral head epiphyseal necrosis in juvenile rabbits," *Current Medical Science*, vol. 38, no. 2, pp. 277–288, 2018.

[2] A. Aimaiti, Y. Saiwulaiti, M. Saiyiti, Y. H. Wang, L. Cui, and A. Yusufu, "Therapeutic effect of osteogenically induced adipose derived stem cells on vascular deprivation-induced osteonecrosis of the femoral head in rabbits," *Chinese Journal of Traumatology*, vol. 14, no. 4, pp. 215–220, 2011.

[3] A. Abudusaimi, Y. Aihemaitijiang, Y. H. Wang, L. Cui, S. Maimaitiming, and M. Abulikemu, "Adipose-derived stem cells enhance bone regeneration in vascular necrosis of the femoral head in the rabbit," *The Journal of International Medical Research*, vol. 39, no. 5, pp. 1852–1860, 2011, PMID: 22117986.

[4] L. Mazini, L. Rochette, M. Amine, and G. Malka, "Regenerative capacity of adipose derived stem cells (ADSCs), comparison with mesenchymal stem cells (MSCs)," *International Journal of Molecular Sciences*, vol. 20, no. 10, p. 2523, 2019.

[5] X. Li, M. Wang, X. Jing et al., "Bone marrow- and adipose tissue-derived mesenchymal stem cells: characterization, differentiation, and applications in cartilage tissue engineering," *Critical Reviews in Eukaryotic Gene Expression*, vol. 28, no. 4, pp. 285–310, 2018, PMID: 30311578.

[6] D. Zhang, N. Ni, Y. Wang et al., "CircRNA-vgll3 promotes osteogenic differentiation of adipose-derived mesenchymal stem cells via modulating miRNA-dependent integrin α5 expression," *Cell Death and Differentiation*, vol. 28, no. 1, pp. 283–302, 2021.

[7] C. Zhang, M. Li, J. Zhu, F. Luo, and J. Zhao, "Enhanced bone repair induced by human adipose-derived stem cells on osteogenic extracellular matrix ornamented small intestinal submucosa," *Regenerative Medicine*, vol. 12, no. 5, pp. 541–552, 2017.

[8] J. Liu, P. Zhou, Y. Long, C. Huang, and D. Chen, "Repair of bone defects in rat radii with a composite of allogeneic adipose-derived stem cells and heterogeneous deproteinized bone," *Stem Cell Research & Therapy*, vol. 9, no. 1, 2018.

[9] H. Zhang, Y. Zhou, N. Yu et al., "Construction of vascularized tissue-engineered bone with polylysine-modified coral hydroxyapatite and a double cell-sheet complex to repair a large radius bone defect in rabbits," *Acta Biomaterialia*, vol. 91, pp. 82–98, 2019.

[10] J. Wei, M. Xu, X. Zhang et al., "Enhanced osteogenic behavior of ADSCs produced by deproteinized antler cancellous bone and evidence for involvement of ERK signaling pathway," *Tissue Engineering. Part A*, vol. 21, no. 11-12, pp. 1810–1821, 2015.

[11] M. Sheykhhasan, J. K. L. Wong, and A. M. Seifalian, "Human adipose-derived stem cells with great therapeutic potential," *Current Stem Cell Research & Therapy*, vol. 14, no. 7, pp. 532–548, 2019, PMID: 30973112.

[12] J. Li, Q. Zhao, E. Wang, C. Zhang, G. Wang, and Q. Yuan, "Transplantation of Cbfa 1-overexpressing adipose stem cells together with vascularized periosteal flaps repair segmental bone defects," *Journal of Surgical Research*, vol. 176, no. 1, pp. e13–e20, 2012.

[13] B. Liu, L. Cui, G. P. Liu, Y. L. Cao, J. T. Zhu, and Y. Cao, "Tissue-engineering bone with ADSCs and coral scaffold for repairing of cranial bone defect in canine," *Zhonghua Zheng Xing Wai Ke Za Zhi*, vol. 25, no. 3, pp. 204–208, 2009.

[14] B. Hashemibeni, E. Esfandiari, F. Sadeghi et al., "An animal model study for bone repair with encapsulated differentiated osteoblasts from adipose-derived stem cells in alginate," *Iranian Journal of Basic Medical Sciences*, vol. 17, no. 11, pp. 854–859, 2014.

[15] T. Guo, X. Tian, B. Li, T. Yang, and Y. Li, "Repair of articular cartilage and subchondral defects in rabbit knee joints with a polyvinyl alcohol/nano-hydroxyapatite/polyamide 66 biological composite material," *Journal of Orthopaedic Surgery and Research*, vol. 12, no. 1, 2017.

[16] Y. Xiong, C. Ren, B. Zhang et al., "Analyzing the behavior of a porous nano-hydroxyapatite/polyamide 66 (n-HA/PA66) composite for healing of bone defects," *International Journal of Nanomedicine*, vol. 13, no. 9, pp. 485–494, 2014.

[17] Y. Zhu, Y. Wu, J. Cheng et al., "Pharmacological activation of TAZ enhances osteogenic differentiation and bone formation of adipose-derived stem cells," *Stem Cell Research & Therapy*, vol. 9, no. 1, p. 53, 2018.

[18] R. Alluri, A. Jakus, S. Bougioukli et al., "3D printed hyperelastic "bone" scaffolds and regional gene therapy: a novel approach to bone healing," *Journal of Biomedical Materials Research. Part A*, vol. 106, no. 4, pp. 1104–1110, 2018.

[19] Q. Le, V. Madhu, J. M. Hart et al., "Current evidence on potential of adipose derived stem cells to enhance bone regeneration and future projection," *World Journal of Stem Cells*, vol. 13, no. 9, pp. 1248–1277, 2021.

[20] M. Ishihara, S. Kishimoto, M. Takikawa, H. Hattori, S. Nakamura, and M. Shimizu, "Biomedical application of low molecular weight heparin/protamine nano/micro particles as cell- and growth factor-carriers and coating matrix," *International Journal of Molecular Sciences*, vol. 16, no. 12, pp. 11785–11803, 2015.

[21] M. Ehlert, A. Radtke, T. Jędrzejewski, K. Roszek, M. Bartmański, and P. Piszczek, "In vitro studies on nanoporous, nanotubular and nanosponge-like titania coatings, with the use of adipose-derived stem cells," *Materials*, vol. 13, no. 7, p. 1574, 2020.

[22] X. Jiang, J. Xiu, F. Shen, S. Jin, and W. Sun, "Repairing of subchondral defect and articular cartilage of knee joint of rabbit by gadolinium containing bio-nanocomposites," *Journal of Biomedical Nanotechnology*, vol. 17, no. 8, pp. 1584–1597, 2021.

[23] Y. Hong, Y. Han, J. Wu et al., "Chitosan modified Fe3O4/KGN self-assembled nanoprobes for osteochondral MR diagnose and regeneration," *Theranostics*, vol. 10, no. 12, pp. 5565–5577, 2020.

[24] H. Chen, Y. Qian, Y. Xia et al., "Enhanced osteogenesis of ADSCs by the synergistic effect of aligned fibers containing collagen I," *ACS Applied Materials & Interfaces*, vol. 8, no. 43, pp. 29289–29297, 2016.

[25] S. Razavi, S. Karbasi, M. Morshed, H. Zarkesh Esfahani, M. Golozar, and S. Vaezifar, "Cell attachment and proliferation of human adipose-derived stem cells on PLGA/chitosan electrospun nano-biocomposite," *Cell Journal*, vol. 17, no. 3, pp. 429–437, 2015.

[26] S. Ma, Z. Wang, Y. Guo et al., "Enhanced osteoinduction of electrospun scaffolds with assemblies of hematite nanoparticles as a bioactive interface," *International Journal of Nanomedicine*, vol. 8, no. 14, pp. 1051–1068, 2019.